

# SCIENCE FOR GLASS PRODUCTION

UDC 666.151:666.1.053.2:620.171.5

## STRESSES AT CRACK APEXES IN GLASS

**L. G. Kopchekchi<sup>1</sup> and L. A. Shitova<sup>1</sup>**Translated from *Steklo i Keramika*, No. 8, pp. 3–5, August, 2001.

---

The forms and types of stressed zones at the apexes of edge cracks depending on the crack size, the presence of the propping liquid, and the existence of post-annealing stresses in glass are investigated. The mechanism for protecting a glass surface from damage using post-annealing stresses is discussed.

---

The service strength of glass amounts to less than 1% of its natural strength, mainly due to cracks arising in glass molding. The state of the cracks depends on the type and the value of stress at crack apexes. Tensile stresses are especially dangerous for glass. Stresses at crack apexes determine the strength of glass.

However, there is as yet no consensus on the distribution of stresses at crack apexes and the effect of glass fluidity on stress distribution. According to the data supplied by Tuba, the remotest point of the maximum stress makes an angle of 69° with the crack growth direction; Rice reports this angle to be 100°, and, according to Kerkhof, this angle is 60° [1–3].

The purpose of the present study was to determine the shape, extent, and type of stressed zones at the apexes of edge cracks depending on the crack length, the presence of stresses in glass after annealing, or the effect of propping liquid in the crack.

The post-annealing stresses extremely complicate the studies of stress fields; therefore, to eliminate their effect, the glass was incised against the end, and the fields were viewed in the normal direction, in which only the stresses along the  $\sigma_x$  and  $\sigma_y$  axes are visible. Upon plane tension stresses along  $z$ -axis equal zero and annealing terminal stresses are unseen.

Incised glass samples of size 70 × 120 × 13 mm were photographed on a reversal color film in polarized light. The photos were made with a Zenit-3M camera with extension rings of the total length up to 175 mm. In this case, the photo camera functions as a microscope with magnification × 2–50.

Polarized light was obtained using a PKS-125 polarimeter. The polarizer being integrated with an analyzer, a dark field becomes visible, in which only the areas with enhanced

stresses glow [4]. To increase the resolving capacity of the polarimeter, a plate was inserted between the polarizer and the analyzer. In this case, the dark field turns purple, which corresponds to “zero” stress, the tensile stresses acquire a sky-blue tint, and the compressive stresses turn red. Such tinting is typical of low-level stresses within the limit of 9 MPa and is very convenient for studying post-annealing stresses. When stresses significantly exceed the specified value, the compression and tension areas acquire identical colors, and only their alternation sequence is modified (Table 1).

To identify the type of stress (tension or compression), an external load was gradually increased, and the alternation of colors in the given glass point was analyzed. After the stress value correlating with the ray path difference 570 nm/cm, the colors alternate again in the same sequence. Glass of thickness 13 mm withstands 6–8 sequences of the compression load and only 3 sequences of the tensile loads. The sequences are interdivided by the dark “zero” lines. The number of lines corresponds to the number of preceding sequences, and the color inside the latest sequence determines the stress value inside this sequence.

The overall stress in the considered point is found from the equation

$$\sigma = 570n + \Delta,$$

where  $n$  is the number of the sequence and  $\Delta$  is the stress inside the latest sequence.

Figure 1a indicates the stressed fields at the apex of a crack whose length exceeds by an order of magnitude the extent of the fields. In this case, the glass edge does not affect the shape and the size of the stressed zones. The sample is subjected to three-point bending by applying a force of 100 N. The distance between the supports is 100 mm.

<sup>1</sup> Saratov Institute of Glass Joint-Stock Company, Saratov, Russia.

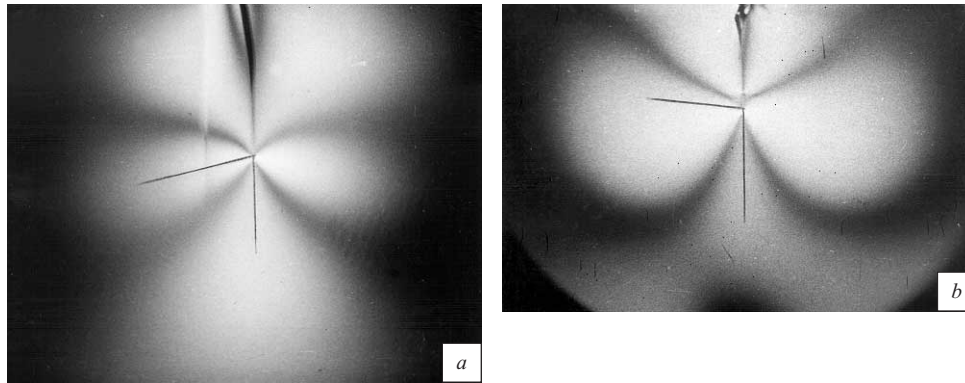


Fig. 1. Stress distribution at a loaded crack apex ( $\times 2$ ) under a load of 100 N (a) and 180 N (b).

The fields are described by the following equations [5]:

$$\sigma_x = \sigma \sqrt{\frac{a}{2r}} \cos \frac{\theta}{2} \left( 1 - \sin \frac{\theta}{2} \sin \frac{3\theta}{2} \right); \quad (1)$$

$$\sigma_y = \sigma \sqrt{\frac{a}{2r}} \cos \frac{\theta}{2} \left( 1 + \sin \frac{\theta}{2} \sin \frac{3\theta}{2} \right), \quad (2)$$

where  $\sigma$  is the external tensile force,  $a$  is the edge crack length,  $r$  is the distance to the crack apex, and  $\theta$  is the angle between the vector  $r$  and the crack direction.

Under the effect of the external force, three compression areas and two tension areas are observed in the crack-apex region. The remotest point of the maximum tension makes an

angle of  $76^\circ$  with the crack-growth direction. As the external load increases, the angle is modified, and under the maximum load before the fracture of the sample (180 N), this angle is equal to about  $100^\circ$  (Fig. 1b).

In accordance with Eqs. (1) and (2), the stresses  $\sigma_x$  and  $\sigma_y$  at the crack apex, where  $r = 0$ , should grow to infinity. In reality, the stresses increase up to a stress whose value is equal to the glass fluidity limit; after that a plastic flow of glass is formed, which unloads the crack.

Plastic flow represents an irreversible deformation; therefore, after the external load is removed ( $\sigma = 0$ ), the stresses  $\sigma_x$  and  $\sigma_y$  are not converted to zero, as required by Eqs. (1) and (2) but change their sign to the opposite one: tensile stresses arise in the sites where compression zones used to be. Three tensile zones are formed at the crack apex: one of them is directed from the crack apex into the glass depth, and two zones are formed on both sides of the crack [6]. Cracking of glass occurs along these directions, forming one median and two lateral cracks, whereas two tensile zones are transformed into compression stresses [7].

The angle between the remotest maximum stress point and the direction of crack growth in the absence of an external load is equal to  $69^\circ$ . For short edge cracks, whose length is smaller by an order of magnitude than the field extension, this angle is  $54^\circ$  (Fig. 2). Thus, the crack length has a substantial effect on the shape of the stressed zone. The proping liquid has an even greater effect on the stressed state of glass with a crack.

Figure 3 shows the same crack that was represented in Fig. 2, but with kerosene penetrating in its apex. The angle is  $90^\circ$ , the same as when applying a critical external load. The stresses are redistributed in such a way that the crack edges are stretched to opposite sides with a force over 30 MPa. A small external effect would be sufficient to break the sample. A specific feature of the stressed state of the crack with the liquid is the altered position of the maximum stress zone.

Whereas in the cases shown in Figs. 1 and 2 all stresses converge in the crack apex, in this particular case the maximum stresses are applied to the crack edges. The water penetrating into the crack from ambient air due to the capillary

TABLE 1

Compression			Tension		
color	ray path difference, nm/cm	stress, MPa	color	ray path difference, nm/cm	stress, MPa
<i>The first sequence</i>					
Purple	0	0	Purple	0	0
Red	+ 25	+ 1.20	Sky-blue	- 115	- 4.80
Orange	+ 130	+ 5.40	Sky-blue-green	- 145	- 6.03
Light yellow	+ 260	+ 10.80	Green	- 200	- 8.35
White			Yellowish-green	- 275	- 11.40
Yellowish-green	+ 325	+ 13.50	Orange	- 485	- 20.20
	+ 375	+ 15.55			
Green	+ 450	+ 18.70	Orange-red	- 525	- 21.80
Sky-blue	+ 565	+ 23.50	Red	- 565	- 23.50
<i>The second order</i>					
Purple	+ 570	+ 23.75	Purple	- 570	- 23.75
Red	+ 595	+ 24.80	Sky-blue	- 685	- 28.50
Orange	+ 700	+ 29.20	Sky-blue-green	- 715	- 29.80
Light yellow	+ 830	+ 34.60	Green	- 770	- 32.00
White	+ 895	+ 37.30	Yellowish-green	- 845	- 35.20
Yellowish-green			Orange	- 1055	- 44.00
	+ 945	+ 39.30			
Green	+ 1030	+ 43.20	Orange-red	- 1095	- 45.60
Sky-blue	+ 1135	+ 47.40	Red	- 1135	- 47.40

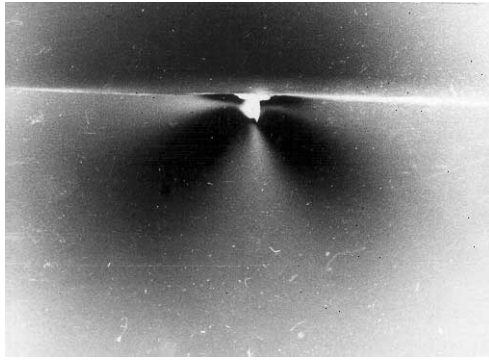


Fig. 2. Stress distribution at an unloaded crack apex ( $\times 10$ ).

condensation forces has the same effect on the crack as kerosene does. The higher the air humidity, the greater the effect of moisture on the crack and, consequently, the greater the angle determined in the measurement. That is why there is as yet no consensus on the shape of the stressed zones at the crack apex. The measurements performed for this particular study were carried out when the relative air moisture was 30%, in which case capillary condensation can be ignored [4].

The field distribution also changes in the presence of post-annealing stresses. Since molded glass is chilled at a fairly high rate, all types of glass have residual post-annealing stresses. The end view of sheet glass is seen as a three-layer composite: orange-colored compression areas are seen on the top and at the bottom, and in the middle there is a tensile area tinted sky-blue. The compression and tension areas are divided between themselves by two "zero" lines.

If glass is damaged, a crack grows via the compressive area and reaches the tensile area with its apex. The glass resists destruction and "pumps" the compressive stress from the surface to the crack apex. The crack cannot grow through a compression area. Consequently, the crack either stops or changes its direction of growth. A typical loop formed by zero stresses limiting the compression area arises in the glass (Fig. 4). For further growth of the crack, the external destructive load should be increased; in this case the compressive stress in the apex first decreases to zero and then transforms into a tensile stress. In general, this is manifested in increased glass strength. Thus, post-annealing compressive stresses protect the glass surface from damage, retard the propagation of cracks, and prevent self-destruction of the glass.

The angle between the remotest maximum stress point and the crack-growth direction is  $54^\circ$  for short edge cracks, whereas for long cracks, in which the edge effect is minimum, this angle grows to  $69^\circ$ .

An increase in external load also brings the angle to its maximum value ( $100^\circ$ ), after which the sample becomes destroyed. The propping liquid acts similarly to the external load and increases the angle to  $90^\circ$ . Air moisture through the capillary condensation force can penetrate into the crack and modify the measurements results. That is why there is no

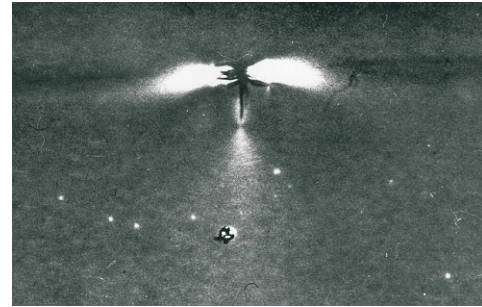


Fig. 3. Stress distribution in the region of a crack with kerosene ( $\times 25$ ).

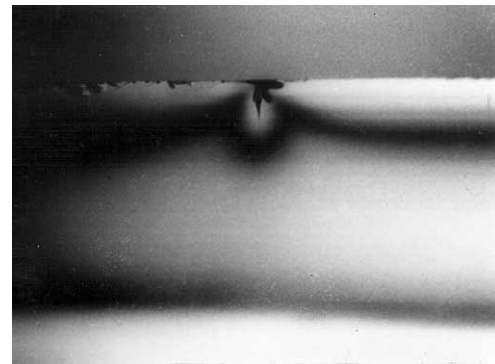


Fig. 4. Stress distribution in a crack apex in the presence of annealing stresses ( $\times 5$ ).

consensus with respect to the shape of stressed zones in the vicinity of a crack.

Thus, when glass with post-annealing stresses is being destroyed, the compressive stress is shifted from the surface into the glass depth. A characteristic loop is formed here, which limits the compression area. In this case, the crack cannot grow into the compression area and stops. Post-annealing compressive stresses protect the glass surface from damage, retard the propagation of cracks, and prevent the self-destruction of glass.

## REFERENCES

1. I. S. Tuba, "A method of elastic-plastic plane stress and strain analysis," *Strain Analysis*, No. 1, 115 – 122 (1966).
2. J. R. Rise and G. F. Rosengren, "Plane strain deformation near a crack tip in a power-law hardening material," *Mech. Phys. Sol.*, **16**, 1 (1968).
3. F. Kerkhof, *Bruchvorgaenge in Glaesern*, Main: Glastechn. Ges., Frankfurt (1970).
4. L. G. Kopchekchi, "Causes of surface damage in thermally polished glass in production," *Steklo Keram.*, No. 5, 6 – 8 (1999).
5. D. Broek, *Principles of Mechanics of Destruction* [Russian translation], Moscow (1980).
6. L. G. Kopchekchi and L. A. Shitova, "Initiation and propagation of cracks in glass beneath a roll cutter," *Steklo Keram.*, No. 4, 11 – 13 (1996).
7. L. G. Kopchekchi and L. A. Shitova, "Dependence of the crack depth on the glass-cutting rate," *Steklo Keram.*, No. 8, 6 – 8 (1999).